Magnetization transfer effects in MR imaging of in vivo intracranial hemorrhage.

R L Mittl, Jr, J M Gomori, M D Schnall, G A Holland, R I Grossman and S W Atlas

AJNR Am J Neuroradiol 1993, 14 (4) 881-891
http://www.ajnr.org/content/14/4/881

Magnetization Transfer Effects in MR Imaging of in Vivo Intracranial Hemorrhage

Robert L. Mittl, Jr., John Moshe Gomori, Mitchell D. Schnall, George A. Holland, Robert I. Grossman, and Scott W. Atlas

PURPOSE: Recent papers have hypothesized that diamagnetic effects of clotting and conformational changes in aging red blood cells immobilize the hemoglobin protein and thus are responsible for the marked hypointensity of acute hematomas on T2-weighted spin-echo MR images. To test that hypothesis, the authors evaluated 24 hemorrhagic components of intracranial hemorrhagic lesions using accepted criteria based on spin-echo images as the definitions of the stage of the hemorrhage. **METHODS:** As a measure of the effects of macromolecular (hemoglobin protein) immobility, magnetization transfer contrast was elicited using a pulsed saturation magnetization transfer experiment. The apparent magnetization transfer contrast (AMTC) was determined by comparing the signal intensities of saturated with unsaturated images and quantified for acute isolated hemorrhages, acute nonisolated hemorrhagic lesions, and subacute-to-chronic hemorrhages. **RESULTS:** The AMTC of isolated acute hemorrhage was significantly less than that of normal white matter and gray matter, indicating the lack of significant magnetization transfer and therefore the lack of effects of restriction of hemoglobin mobility on the signal intensity of acute hemorrhage. Acutely hemorrhagic tissue (nonisolated acute hemorrhage) has significantly more AMTC than isolated acute hemorrhage, but still not exceeding that of brain parenchyma. **CONCLUSION:** This in vivo data concurs with in vitro data and reinforces the concept that the marked hypointensity of acute hematomas is mainly a magnetic susceptibility effect.

Index terms: Hematoma; Cerebral hemorrhage; Blood, coagulation; Blood, magnetic resonance; Magnetic resonance, tissue characterization

AJNR 14:881–891, Jul/Aug 1993

Evolving intracranial hemorrhage on magnetic resonance (MR) imaging follows a typical pattern (1). Despite the complex nature of this entity, the relaxation enhancement caused by the heme-associated iron in hematomas has generally been accepted as the major determinant to signal intensity patterns of hematomas on spin echo images (1–16). The magnetic susceptibility effects of deoxyhemoglobin in particular have been shown to be of critical importance to the characteristic signal intensity pattern of acute hematomas at 1.5 T, which is isointense to brain on short repetition time (TR)/short echo time (TE) images and markedly hypointense on long TR/long TE images. This hypointensity has been attributed to the T2 shortening from magnetic field inhomogeneity produced when deoxyhemoglobin is compartmentalized within red blood cells (1, 17, 18). Other factors, such as hemoglobin and serum protein concentration and fibrin polymerization also have been investigated as contributors to the signal characteristics observed in different stages of hemorrhage (19–21). A recent report suggested that the significance of magnetic susceptibility variations to the production of marked hypointensity on long TR/TE spin-echo images in acute hematomas may have been overestimated (22). These authors proposed that the immobolization of hemoglobin in hematomas by clotting and conformational changes in the red blood cell may, in fact, compose a major T2 shortening mechanism (19, 20, 22).

Magnetization transfer recently has received increasing attention in the literature as a potentially important mechanism in MR image contrast (23–26), although the concept is based on pre-

Received July 22, 1992; revision requested December 29, received February 1, 1993, and accepted February 11.

All authors: Department of Radiology, Hospital of the University of Pennsylvania, 3400 Spruce Street, Philadelphia, PA 19104. Address reprint requests to Scott W. Atlas, MD.

AJNR 14:881–891, Jul/Aug 1993 0195-6108/93/1404-0881

vious work studying cross-relaxation phenomena (27–29). This concept refers to the observation of enhanced relaxation of free water protons caused by the exchange of magnetization from immobile protons of macromolecules to unbound water protons. The magnetization transfer from macromolecular-bound protons to free water protons is actually a two-step process, in that the transfer (probably a dipolar interaction) (30) involves the macromolecular protons and a transient 'boundary layer' pool of protons, water that is temporarily bound to macromolecules but rapidly exchanges by diffusion with the larger pool of free water (23). This phenomenon has been shown to occur in many diverse tissues (23, 24, 26), including cerebral white matter, where the restricted motion of protons bound to cellular macromolecular structures (postulated to be related to cholesterol-containing lipid bilayers of myelin) significantly influences the relaxation rates of unbound water by this process (31). Magnetization transfer contrast (MTC) can be demonstrated by applying a high-power radio frequency pulse away from the resonance peak of free water protons to selectively saturate the broad resonance of immobile protons associated with macromolecules. If magnetization transfer occurs, partial saturation as manifested by loss of signal will be observed in the nonirradiated pool of free water spins. The extent of apparent magnetization transfer contrast can be quantified by comparing the signal intensity of saturated with unsaturated images.

Immobilization of protein macromolecules increases the population of restricted spins, and so it increases the amplitude of the broad resonance component. Such an increase in the population of restricted spins will increase the MTC. In addition, an increase in macromolecular immobility will shorten T2 by a separate mechanism (30). Importantly, the magnetization transfer phenomenon is not sensitive to susceptibility-induced relaxation, unlike T2 relaxation (32). Therefore, the magnetization transfer experiment is an ideal way to separate magnetic susceptibility effects from transverse relaxation due to the immobilization of macromolecules. The effects of restriction of hemoglobin mobility, as proposed for acute hematomas (19, 22), should be revealed by a pulse sequence sensitive to magnetization transfer. Our study is also prompted by a separate study of hepatic lesions, in which Outwater et al (26) showed that liver hemangiomas, which are to a great extent composed of blood in vascular spaces admixed with internal stroma, demonstrate considerably more magnetization transfer than simple fluids, such as water and cerebrospinal fluid. The purpose of our study was to investigate the effects of macromolecular immobility on the signal intensity of in vivo intracranial hematomas.

Subjects and Methods

Seventeen patients with intracranial hemorrhage as documented by spin-echo images were evaluated, including four patients with two separate lesions. Twenty-four separate hemorrhage components were identified in 21 hemorrhagic lesions. All studies were performed on a 1.5-T MR system (Signa, GE Medical Systems, Milwaukee, WI). Spin-echo pulse sequences were performed before the evaluation of magnetization transfer. Sagittal and/or axial conventional spin-echo short TR/TE (500–800/12–26) and axial long TR/short and long TE (2500–4000/18–30 and 80–90) dual-echo spin-echo pulse sequences were performed on all patients. The long TR images in six patients were performed using a fast spin-echo pulse sequence previously described elsewhere (33, 34) rather than conventional spin-echo imaging. We realize that this sequence is less sensitive to magnetic susceptibility effects than conventional spin-echo sequences because of the inherently short interval between consecutive 180-degree rf pulses. Clearly, however, this would not lead to *false-positive* identification of deoxyhemoglobin, which was defined in this study as marked hypointensity on long TR/long $TE_{effective}$ images (where $TE_{effective}$ refers to the echo delay at which the low spatial frequencies, which are responsible for the contrast, were acquired for the fast spin-echo image). On the other hand, there is certainly a possibility of missing a lesion (ie *false-negative* fast spin-echo scan) containing deoxyhemoglobin, because of reduced prominence of the characteristic hypointensity of acute hemorrhage on fast spin echo images.

The stages of hemorrhage were based upon previously described and widely accepted signal intensity patterns on spin-echo images at 1.5 T (1). Acute hemorrhage was defined as slightly hypointense or isointense to brain on short TR/short TE images and markedly hypointense on long TR/long TE (or long TR/long $TE_{effective}$) images. Subacute-to-chronic hemorrhage was defined as hyperintense on short and long TR/TE images.

Magnetization transfer contrast was generated by using a pulsed saturation technique based upon a previously described pulse sequence (35). which modifies the fat saturation pulse in a standard three-dimensional gradient echo sequence (GRASS; GE Medical Systems). Parameters included a TR of 106 msec, a TE of 5 msec, and a flip angle of 12 degrees. A nonsection-selective saturation pulse was applied 2 kHz below the resonance peak of free water to selectively saturate the broad resonance of the pool of immobile protons of macromolecules. The saturation pulse consisted of a 19-msec single-cycle sinc pulse with an

average B_1 intensity of 3.67×10^{-6} T. The interval between the saturation pulse and the excitation pulse was approximately 1 msec. Without changing prescan values or slice selection, an unsaturated series of images was also acquired by using the identical pulse sequence without the saturation pulse. Details of this pulse sequence have been described elsewhere, and notwithstanding the known pulse sequence dependence of the quantified magnetization transfer effect, its reproducibility has been validated in previous studies (25, 26).

Analysis of the images was performed by consensus by two neuroradiologists who inspected the spin-echo images to identify the stage of blood in each lesion and in different portions of each lesion. The stage of blood evaluated was defined by well-described criteria observed for evolving hematomas at 1.5 T (1). Regions of interest (ROIs) were subsequently defined on the corresponding portions of the magnetization transfer images in homogeneous areas where confident identification of blood components could be made and where volume averaging effects could be avoided. Extreme care was taken to avoid partial volume effects when selecting ROIs in the regions of hemorrhage by selecting ROIs in lesions that were also demonstrated on sections immediately above and below the section from which measurements were taken. Two to four separate ROIs were selected for each component of the hemorrhages, and these values were averaged. Identical ROIs were selected on the saturated and unsaturated MT images. The magnitude of signal intensity with the saturation pulse on and the magnitude of signal intensity with the saturation pulse turned off were used to determine the degree of magnetization transfer. An apparent MTC (AMTC) was obtained with this equation:

$$\text{AMTC} = \frac{\text{signal intensity (unsat)} - \text{signal intensity (sat)}}{\text{signal intensity (unsat)}}. \quad (1)$$

We chose to measure the AMTC rather than the magnetization transfer rate (MTR) because there are significant constraints to accurately measuring the MTR. First, it is necessary to employ the continuous wave saturation method (24), which uses continuous saturation with incremental increases in saturation time (duration), to accurately measure the MTR. This method, although potentially accurate for determining the MTR, is limited by power absorption limitations on B_1 and radiofrequency pulse bleed-over (ie inadvertant saturation of the free water resonance by the saturation pulse). Second, when using our pulsed saturation method, there is a limit to the achievable saturation of the immobile macromolecular protons. Importantly, it should be noted as well that the AMTC is highly dependent upon the T1 relaxation time, such that

$$\text{AMTC} = T1_{sat} \cdot \text{MTR}, \quad (2)$$

where $T1_{sat}$ represents the T1 relaxation time of free water protons under conditions of magnetization transfer assuming complete saturation of the immobile protons and no radiofrequency pulse bleed-over.

AMTC values were obtained in all patients for cerebrospinal fluid and for normal appearing white matter and normal appearing gray matter (putamen) to serve as intrapatient controls. The Student *t* test (unpaired two-tail) was used for statistical analysis, and a *P* value less than 0.05 was considered statistically significant.

Results

AMTC values for cerebrospinal fluid, normal-appearing white matter, and normal-appearing deep gray matter (putamen) were obtained in all patients. The mean AMTC for cerebrospinal fluid was 0.006 (SD = 0.019) with a range from −0.040 to 0.028. The AMTC values for cerebrospinal fluid in ideal conditions should equal zero. The nonzero values for cerebrospinal fluid in our study (as in previous investigations using this technique) reflect a minimal radio frequency bleed-over from the off-resonance saturation pulse onto the resonance of free water protons (26). The mean AMTC for normal-appearing white matter was 0.412 (SD = 0.023). These values are very similar to the values for AMTC of normal-appearing white matter previously reported for healthy volunteers that were obtained using the same pulse sequence used in this study (25). The mean AMTC of normal-appearing gray matter was 0.360 (SD = 0.026). The difference between the AMTC between normal-appearing white matter and gray matter was statistically significant ($P = 0.0001$). We note that the AMTC values for gray matter and white matter differ somewhat from those reported in our in vitro investigation (36), which can be ascribed to the slight difference in flip angle used in the two studies.

Twenty-four separate hemorrhagic components in 21 hemorrhagic lesions were studied in 17 patients (note that some lesions had more than one type of hemorrhagic component). Table 1 lists the age and sex of each patient as well as the nature of each hemorrhagic lesion (see Table 2 for statistical comparisons). The mean AMTC for subacute-to-chronic hemorrhage with extracellular methemoglobin (as defined by regions of high intensity on short TR/TE and long TR/TE spin-echo images) measured in 12 lesions was 0.073 (SD = 0.038) with a range from 0.036 to 0.134. The mean AMTC for acute hemorrhage with intracellular deoxyhemoglobin (as defined by regions of isointensity or slight hypointensity on short TR/TE and marked hypointensity on long TR/TE spin-echo images) measured in 9 lesions was 0.266 (SD = 0.096) with a range from

TABLE 1: Apparent magnetization transfer contrast for intracranial hemorrhagic lesions

Patient	Age/Sex	Lesion(s)	High SI on Short TR/TE and Long TR/TE Images (Extracellular MetHgb)	Slight Low SI on Short TR/TE and Marked Low SI on Long TR/TE Images (Intra cellular DeoxyHgb)	Isointense on Short TR/TE and Slight High SI on Long TR/TE Images (Hyperacute Hematoma)
CB	65/F	Sinus thrombosis with a hemorrhagic infarct		0.338	
HC	56/M	Hemorrhagic metastases			
		Lt parietal	0.053	0.115[a]	
		Parasagittal		0.250	
JC	75/M	Occipital hemorrhage, probably due to HTN	0.094		
MC	45/M	Hemorrhagic AVM		0.155[a]	0.186
NC	80/F	Subdural hematoma	0.074		
JE	50/M	Probable OCVMs:			
		Left temporal	0.038		
		Cerebellar	0.058		
AF	47/M	Left basal ganglia hemorrhage, probably due to HTN	0.108		
DG	74/F	Hemorrhagic thalamic metastasis		0.341	
GG	66/F	Hemorrhagic cerebellar metastasis	0.054	0.376	
VG	23/F	Hemorrhagic temporal OCVM	0.134		
HH	48/M	Hemorrhagic metastases:			
		Rt parietal		0.285	
		Lt parietal	0.084		
MM	37/M	Subdural hematoma	0.110		
JR	72/M	Left temporal hemorrhage, HTN	0.038		
JS	47/F	Left temporal hemorrhage, ?Etiology		0.357	
SS	82/M	Rt parietal hemorrhage, probably amyloid angiopathy	0.115		
NT	73/F	Cerebellar hemorrhage	0.036		
		Subdural hematoma	0.019		
GW	32/F	Hemorrhagic tectal OCVM		0.180[a]	
		Mean	0.073	0.266	0.186
		SD	0.038	0.096	

[a] Debris-fluid level present within lesion indicating isolated blood into cystic cavity.

TABLE 2: Comparison of AMTC values versus AMTC of acute hemorrhage

	(mean) AMTC	*P* value versus $AMTC_{isolated\ acute\ hemorrhage}$[a]	*P* value versus $AMTC_{nonisolated\ acute\ hemorrhage}$[a]
Hyperacute heme	0.186	0.442	0.0428
Isolated acute heme	0.150	N/A	0.0001
Nonisolated acute heme	0.325	0.0001	N/A
Subacute-chronic heme	0.073	0.0034	0.0001
Normal white matter	0.412	0.0001	0.0001
Normal gray matter	0.360	0.0001	0.0264
Cerebrospinal fluid	0.006	0.0001	0.0001

[a] *P* value for two-tailed, unpaired *t* test using raw data for each case.

0.115 to 0.376. Comparison of these mean values demonstrated a statistically significant difference ($P < 0.001$).

Three of the lesions containing deoxyhemoglobin as defined by spin-echo intensities demonstrated debris-fluid levels on spin-echo images (indicated by superscript letters in Table 1), documenting that blood in these lesions was isolated within a cystic cavity (Fig. 1). Two of these lesions were hemorrhages associated with vascular malformations and one was a hemorrhage associated with metastases. The deoxyhemoglobin in these

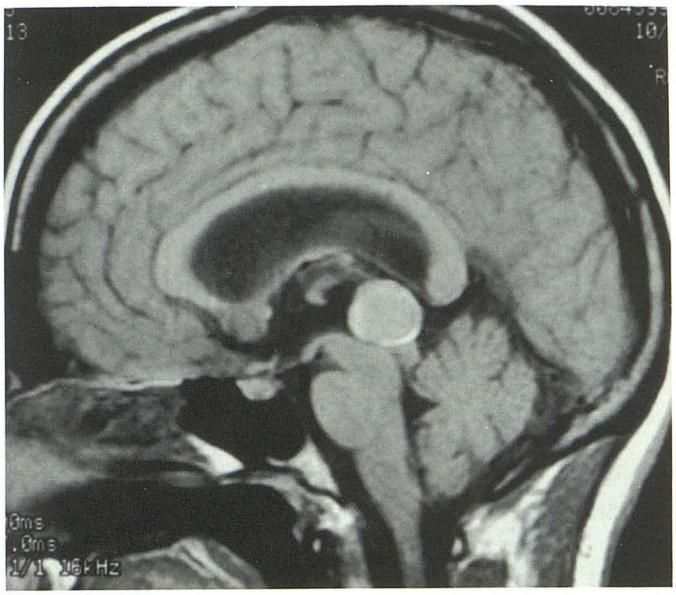

A

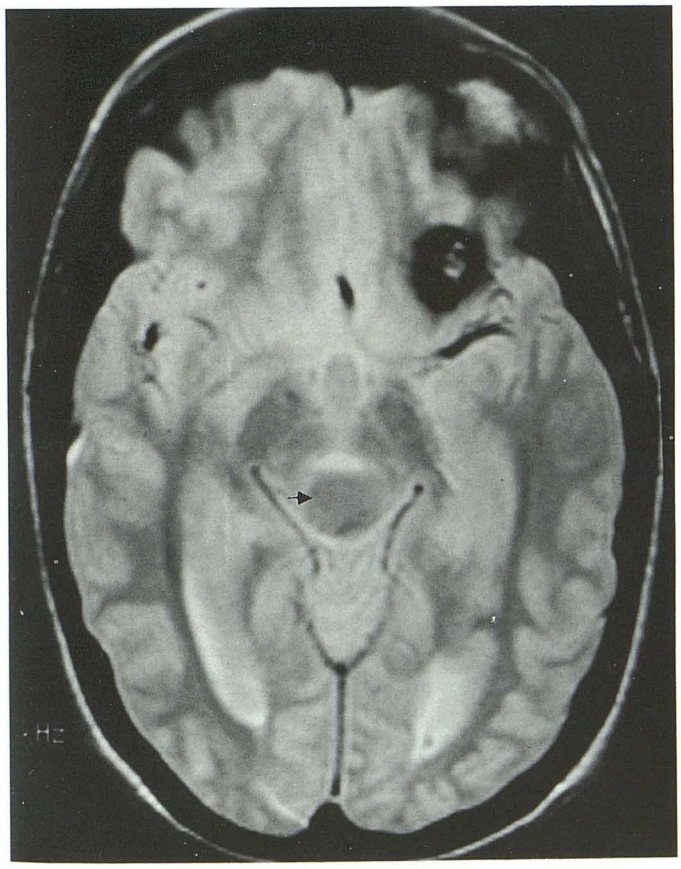

B

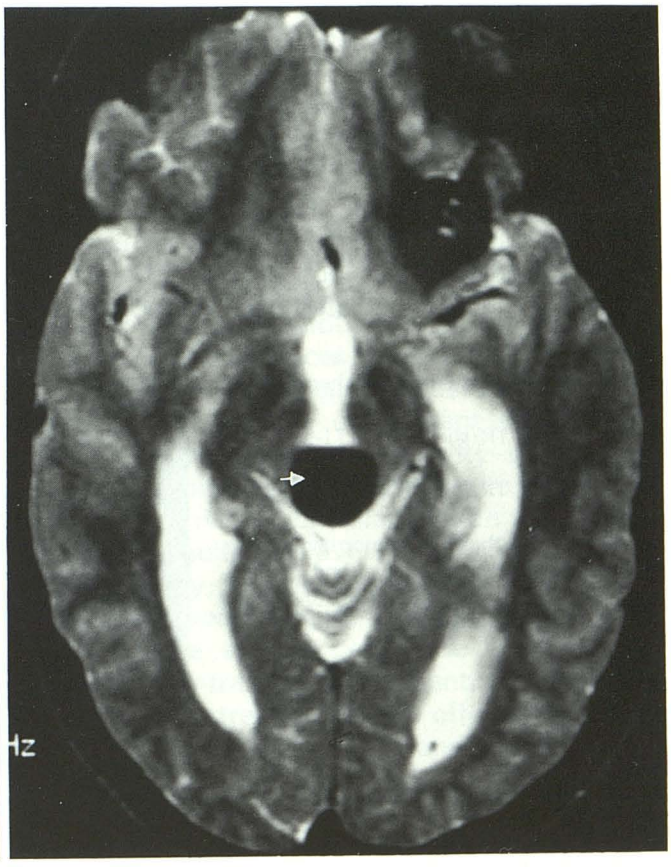

C

Fig. 1. Acute isolated hemorrhage.
A, Short TR/short TE (T1-weighted) image.
B, Long TR/short TE (proton density-weighted) image.
C, Long TR/long TE (T2-weighted) image.
Note dependent debris-fluid level in tectal lesion (*A–C*), with acute hemorrhage consistent with intracellular deoxyhemoglobin in dependent portion (*arrow*). The presence of such a level allows separation of blood component from any other tissue. The second cavernous hemangioma is present in left frontal lobe (*B* and *C*).

cases (what we termed isolated deoxyhemoglobin) had the three lowest AMTC values among the group of hemorrhagic lesions containing deoxyhemoglobin, with a mean AMTC of 0.150 (SD = 0.033). The other six deoxyhemoglobin-containing lesions did *not* demonstrate debris-fluid levels, so the blood could not be separated from underlying solid tissue in these cases (Fig. 2). This group of six nonisolated hemorrhagic tissue cases included four acute hemorrhages due to metastases and two nonneoplastic parenchymal hemorrhages. The mean AMTC for deoxyhemoglobin admixed with underlying tissue (nonisolated deoxyhemoglobin) equaled 0.325 (SD = 0.047). There was a statistically significant difference between the AMTC of the two subgroups of deoxyhemoglobin-containing lesions ($P < 0.001$). The AMTC of *isolated* deoxyhemoglobin was significantly less than the AMTC of normal-appearing white matter ($P = 0.0001$) and gray matter ($P = 0.0001$). The AMTC of *nonisolated* deoxyhemoglobin was not significantly different from the mean AMTCs of normal-appearing white matter ($P = 0.412$) and gray matter ($P = 0.360$) (see Table 2).

One early acute hemorrhagic lesion proved by computed tomography (CT) associated with an arteriovenous malformation had an isointense signal with WM on short TR/short TE images and was slightly hyperintense on long TR/long TE images. This lesion matched descriptions of "hyperacute" hemorrhage (10, 16) by its spin-echo signal intensity pattern. This single case had an AMTC value of 0.186. The AMTC of this hyperacute hematoma was not significantly different from the AMTC of isolated deoxyhemoglobin.

Discussion

The appearance of intracranial hemorrhage on MR imaging is complex, and as a result it has been the subject of numerous investigations. As in the case of all lesions depicted by MR imaging, the concentration of water (spin density) and the relaxation characteristics of the water determine the signal intensity of hemorrhage. Many physiologic factors inherent to the specific hemorrhage, such as the oxygenation state of hemoglobin, hematocrit, and the presence of certain underlying lesions, are well known to influence the MR appearance. Operator-dependent variables, such as the magnetic field strength of the scanner, specific pulse sequence parameters (eg TR, TE, and interecho time), and mechanism of signal acquisition used (radio frequency pulse-induced spin echo versus gradient recalled echo) also influence the observed MR signal intensities to a considerable degree (1–16, 37).

The signal intensities observed in acute hematomas at high field are determined mostly by compartmentalization of deoxygenated hemoglobin within intact red blood cells (1, 14, 17, 18). The compartmentalization of the paramagnetic ferrous iron of deoxyhemoglobin creates regions of inhomogeneous magnetic susceptibility through which diffusing water protons traverse. These local magnetic field inhomogeneities experienced by water protons shorten the apparent T2 leading to hypointensity on long TR/long TE images, particularly at high-field strengths, long TE, and long interecho time (18). Notwithstanding the uncertainty regarding the precise localization of the magnetic susceptibility gradients in acute hematomas (ie transcellular, intercellular,

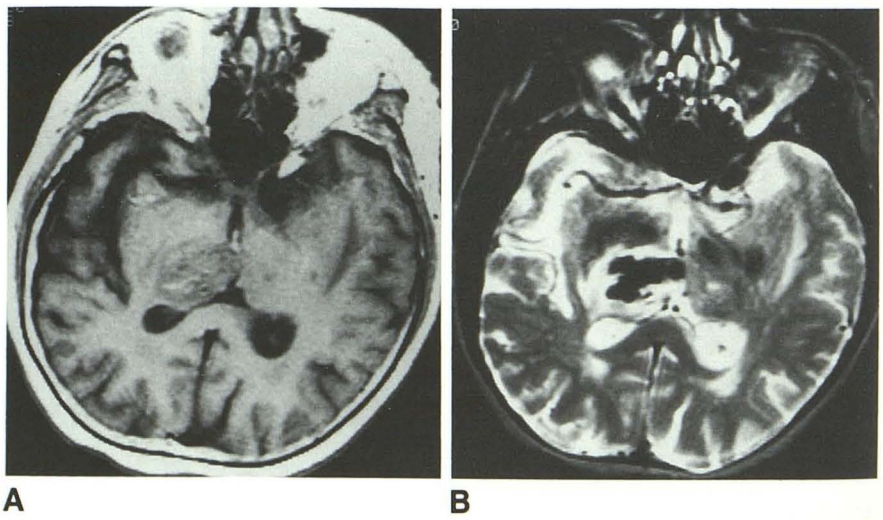

Fig. 2. Acute nonisolated hemorrhagic lesion.

A, Short TR/short TE (T1-weighted) image.

B, Long TR/long TE (T2-weighted) image.

Acute right thalamic hemorrhage shows no definable debris-fluid level and is therefore not clearly separable from underlying (intermixed) brain tissue.

and/or intracellular) (38), it has been shown that lysis of red blood cells is associated with disappearance of the T2 shortening (17, 18). It is presumed that the quarternary structure of deoxyhemoglobin isolates the iron atom and prevents dipole-dipole interactions between it and free water protons, so no T1 shortening is observed. Subsequent conformational changes produced by conversion (ie oxidation) to methemoglobin in subacute hematomas make iron atoms more accessible to water protons. This allows dipole-dipole interactions between water protons and the paramagnetic ferric iron of methemoglobin, and thus high intensity is seen on short TR/short TE images of these lesions.

Many processes occur during clot formation in addition to deoxygenation, including fibrin polymerization, clot retraction, and hemoconcentration. Clark et al (14) investigated the relative effects of these processes on T2 shortening in acute hematomas. In spite of their methodologic design of using very short interecho times, which minimized the effects of magnetic susceptibility-induced T2 shortening, they still found that deoxygenation was the most important determinant of T2 shortening, followed to a lesser extent by increased hematocrit. The effect of fibrin-clot formation was minimal at the high-field strengths examined. Other investigators have postulated that nonparamagnetic protein effects may be highly significant in generating the marked, selective hypointensity on long TR/long TE spin-echo images (19, 20, 22). These authors have stated that conformational changes in red blood cell morphology, intracellular water concentration, and restriction of protein (hemoglobin) mobility in the absence of paramagnetic iron effects are responsible for the intensity pattern of acute hematomas.

Magnetization transfer has received attention recently as an important contrast mechanism in MR imaging (23, 24). This involves the exchange of magnetization between two separate populations of protons—free water protons and the immobile hydrogen protons covalently bound to biologic macromolecules and membranes in tissues. Experimentally, the presence of magnetization transfer can be investigated by the saturation transfer technique (23), in which the selective saturation of macromolecular protons are achieved via rf irradiation distant from the narrow water resonance but encompassing the broad resonance of these bound protons. Subsequent to such selective irradiation, one can detect partial suppression (via saturation) of free water signal. In addition to the observed reduction in signal intensity of the free water pool with saturation of the restricted proton pool, there is also a decrease in the observed T1 of the free water spins. In the absence of inadvertant rf irradiation of the free water resonance, the resultant decrease in free water signal implies transfer of the saturation, that is, magnetization transfer (23, 24). The exchange of energy between the two spin populations is thought to be a dipole-dipole interaction rather than a chemical exchange from observations made using other isotopes of water (eg tritium) (30). This technique is a sensitive method of detecting the effects of immobile macromolecules on water relaxation. Clearly, if essentially no free water is present, then no magnetization transfer could occur. Relaxation induced by magnetization transfer appears to generate contrast separate from conventional determinants of T1 and T2 relaxation rates. In fact, several investigators have suggested that the contrast generated via such magnetization transfer may be useful in clinical brain imaging, both for improving gray-white discrimination (39) and in parenchymal disease (40).

The magnitude of the signal decrease of free water protons is related to the rate of magnetization transfer and to the spin lattice (T1) relaxation time of free water under conditions of steady state saturation of the immobile pool (24), expressed in the following equation:

$$MTR \cdot T1_{sat} = MTC.$$

In distinction to the influence of T1 on MTC measurements, it should be noted that the measurement of MTC is not affected by magnetic susceptibility differences, unlike T2 measurements (32). These unique characteristics of the magnetization transfer experiment (its lack of influence by magnetic susceptibility–induced relaxation) coupled with its sensitivity to the effects of restricted macromolecular motion makes this method well suited to investigate hemorrhage.

In our study, we have chosen to express the MTC as an *apparent* MTC, because the MTC will vary with the specific technique used for the magnetization transfer experiment, including the duration and strength of the off-resonance B_1 field used for saturation (24) and the effects of bleed-over (inadvertant saturation of the free water resonance). We know that AMTC images, representing ratios of saturated and unsaturated data, will not accurately represent the quantita-

tive magnetization transfer effect, because the T1 times of the free and immobile spin populations (ie the $T1_{sat}$) is not taken into account by the AMTC. Despite these shortcomings of AMTC and the fact that some investigators have successfully produced "magnetization transfer rate maps" from MTR and T1 data (24), we agree with their caveats that the time and power deposition liabilities may limit the practicality of quantifying MTR. Although an AMTR measurement can be obtained (36), clinical time constraints may limit its routine use in ill patients. Therefore, we chose to evaluate AMTC in our study.

Almost no magnetization transfer is observed in simple fluids such as water and CSF, which contain little or no macromolecules, no tissue structure, and have relatively small T1/T2 ratios. Our results agreed with this principle, as almost no magnetization transfer was noted for CSF in our patients ($AMTC_{CSF} = 0.006$) or in other simple fluids in previous reports using the same technique (26). Tissues such as brain parenchyma differ from simple fluids and from solutions of similar protein concentrations in their T1/T2 ratio, because macromolecular cellular structures in tissues decrease T2 more than T1 (41, 42), giving tissues a higher T1/T2 ratio. In tissues, the higher the T1/T2 ratio, the more the magnetization transfer effect (43). Previously reported work using $MnCl_2$ solution phantoms constructed to approximate tissue T1/T2 ratios (26) showed that the AMTC did not increase to the expected values. These data indicate that solutions do not equate with tissues, even in the presence of similar T1/T2 ratios, a concept reinforced by our in vitro work (36) demonstrating that in vitro compact-retracted blood clots behave like protein solutions rather than tissues in this regard. We also note low AMTC of the in vivo entity analogous to the in vitro packed clot (the hyperacute hematoma examined in our study).

Our data demonstrate only minimal magnetization transfer in subacute-to-chronic hematomas (ie extracellular methemoglobin) (mean AMTC = 0.073). This finding likely reflects two separate features of the biophysical changes that occur in subacute-to-chronic hemorrhagic lesions. Importantly, it is clear that in the presence of the short T1 (estimated at 740 msec) (6) of subacute-chronic hematomas at 1.5 T, from Equation (2) we note that the AMTC will be reduced. Conceptually, T1 relaxation and relaxation due to saturation transfer can be thought of as competing processes. The effects of saturation transfer (ie the signal decrease) are opposed by T1 relaxation. A high T1 relaxation rate will result in a lower steady state saturation of the free water protons, resulting in a lower AMTC measurement. It should be noted that the reported T1 values for subacute-to-chronic hematomas are similar to white matter (6, 44), but subacute-to-chronic hemorrhage has a much smaller T1/T2 ratio (approximately half) than that of white matter (6). Tissue structure is obviously lacking in these hematomas, reflected clearly by the AMTC of WM being significantly greater than subacute-to-chronic hemorrhage. In an in vitro study (36), the AMTR was quantified in methemoglobin within and after lysis of packed red blood cells and compared to AMTR in deoxyhemoglobin and carbonmonoxyhemoglobin. The in vitro data indicate that there was no significant difference in the AMTRs caused by the presence of paramagnetic methemoglobin or deoxyhemoglobin. Our data are consistent with these concepts. Second, in subacute-to-chronic methemoglobin-containing hematomas, red blood cells lyse, fibrin and methemoglobin are broken down, and the remaining methemoglobin is markedly diluted (45). The result is a high spin-density lesion (ie, high free water concentration, low protein concentration) (6). Relatively minimal transfer would be expected in lesions in which macromolecules have been diluted and degraded. In fact, one may postulate that the AMTC is to some extent falsely elevated because of rf bleedover, which would lead to overestimation of the effect of magnetization transfer.

We identified two discrete subgroups of lesions containing deoxyhemoglobin, even though they showed identical spin-echo signal intensities. Isolated acute hemorrhage into cystic cavities, as documented by the presence of dependent debris-fluid levels, had a mean AMTC of 0.150. This is similar to the in vitro values for deoxyhemoglobin in samples of clotted packed red blood cells (36), even though these entities are inarguably not equivalent. The mean AMTC of the in vivo acute isolated hemorrhages were significantly less than that of normal white matter and normal gray matter (see Table 2). The AMTC of the in vivo acute isolated hemorrhages was equivalent to the AMTC of the hyperacute hematoma, a lesion which is actually hyperintense to brain on long TR/long TE images. Similarly, the in vitro data (36) indicates that the AMTR of diamagnetic packed red blood cells was not significantly different from the AMTR of paramagnetic methe-

moglobin or deoxyhemoglobin. Our in vivo data clearly demonstrate the *lack* of significant magnetization transfer in acute isolated intracranial hemorrhage. These findings indicate that the marked hypointensity on long TR/long TE images in acute hematomas is not due to restricted mobility of the hemoglobin protein and in fact concur with prior investigations (14, 18, 46) and our in vitro study (36) in that the magnetic susceptibility effects of paramagnetic deoxyhemoglobin dominate its spin-echo MR appearance.

Our data also reveal a second group of deoxyhemoglobin-containing lesions. These hemorrhagic lesions did not demonstrate dependent debris-fluid levels, indicating that blood was inseparable from and intermixed with underlying tissue (eg infarcted brain parenchyma or neoplastic tissue). The deoxyhemoglobin in these cases of nonisolated acute hemorrhage demonstrated a significantly higher mean AMTC of 0.325 ($P < 0.001$), as compared with isolated pure deoxyhemoglobin. This degree of magnetization transfer in nonisolated acute hemorrhage is also much greater than that reported in vitro using packed deoxygenated red blood cells with a similar technique (36). In fact, the AMTC of nonisolated acute hemorrhages was similar to (but still less than) AMTC of gray matter and white matter (Table 2) in our study and in previous investigations using our specific pulsed saturation experiment (25). We hypothesize that unavoidable inclusion (partial volume averaging) of brain or diseased tissue intermixed with deoxyhemoglobin, despite being invisible on inspection of spin echo images elevated the observed AMTC in these cases.

This data has possible implications regarding the distinction of hemorrhagic lesions with underlying pathologic tissue from simple, isolated hematomas. Since our data suggest that isolated ("pure") deoxyhemoglobin demonstrates less magnetization transfer than solid lesions containing deoxyhemoglobin, the magnetization transfer experiment may be useful in assessing the extent of tissue comprising a hemorrhagic lesion. We hypothesize that hemorrhagic lesions which tend to create a cavity and result in simple hematomas could potentially be distinguished from other etiologies of hemorrhage that tend to contain blood breakdown products admixed with tissue ranging from hemorrhagic infarctions to hemorrhagic tumors. This is analogous to the application of magnetization transfer to the distinction of benign from malignant liver lesions reported recently (26). One obvious pitfall is the fact that hemorrhagic neoplasms commonly produce cavities (cystic necrosis) with debris-fluid levels on MR (37). Further investigation is needed to determine whether the magnetization transfer technique would be useful in suggesting the etiology of unexplained acute intracranial hemorrhage.

Our observations may also have implications for the appearance of intracranial hemorrhage on low field strength imaging systems. Although susceptibility effects on spin-echo MR are proportional to the square of the magnetic field strength (17, 18), hypointensity has been observed on long TR/long TE images at field strengths as low as 0.17 T (47). This fact has raised the possibility that nonparamagnetic protein effects may be more important determinants of T2 shortening on low field strength systems, simply because of the insensitivity of low field imaging to magnetic susceptibility effects. Clark et al (14), while demonstrating that deoxygenation was the major determinant of T2 shortening in acute hematomas at 2.1 T and 9.4 T, also proposed that nonparamagnetic protein effects may be more important at lower field strengths based on the trends in their data. Despite their methodologic design, which overestimated nonparamagnetic contributions of to T2 shortening, they found that hemoglobin concentration was a more important nonparamagnetic effect than fibrin cross-linking. The lack of importance of fibrin clot formation and retraction are in accordance with the in vitro investigations of magnetization transfer by Gomori et al (36), which demonstrate that fibrin clot polymerization and marked increases in protein concentration do not have the AMTR of brain parenchyma. Aside from magnetic susceptibility effects (although diminished as compared to high field), transverse relaxation related to macromolecular immobility from admixed pathologic tissue (as in our nonisolated hematomas) could lower signal intensity. Clearly, macromolecular immobility alone, however, would certainly not result in more hypointensity than normal brain. At low field, the appearance of acute hemorrhage is strongly influenced by the relaxation behavior of admixed brain (or lesion) tissue and to a lesser extent hemoglobin concentration, but susceptibility effects are less evident than at high field.

Conclusions

We evaluated 24 hemorrhagic components of intracranial hemorrhagic lesions using accepted

criteria based on spin-echo images as the definitions of the stage of the hemorrhage. As a measure of the effects of macromolecular (hemoglobin) immobility, magnetization transfer contrast was elicited generated by a pulsed saturation magnetization transfer experiment and quantified using the AMTC for acute isolated hemorrhages, acute nonisolated hemorrhagic lesions, and subacute-to-chronic hemorrhages. The AMTC of isolated acute hemorrhage was significantly less than that of normal white matter and gray matter, indicating the lack of significant magnetization transfer and, therefore, the lack of effects of restriction of hemoglobin mobility, on the signal intensity of acute hemorrhage. This in vivo data concurs with in vitro data and reinforces the concept that the marked hypointensity of acute hematomas is mainly a magnetic susceptibility effect.

References

1. Gomori JM, Grossman RI, Goldberg HI, Zimmerman RA, Bilaniuk LT. Intracranial hematomas: imaging by high-field MR. *Radiology* 1985;157:87–93
2. Gomori JM, Grossman RI, Bilaniuk LT, et al. High-field MR imaging of superficial siderosis of the central nervous system. *J Comput Assist Tomogr* 1985;9:972–975
3. Gomori JM, Grossman RI, Goldberg HI, et al. Occult cerebral vascular malformations: high field MR imaging. *Radiology* 1986;158:707–713
4. Bradley WGJ, Schmidt PG. Effect of methemoglobin formation on the MR appearance of subarachnoid hemorrhage. *Radiology* 1985;156:99–103
5. Atlas SW, Mark AS, Gomori JM, Grossman RI. Intracranial hemorrhage: gradient echo imaging at 1.5T. Comparison with spin-echo imaging and clinical applications. *Radiology* 1988;168:803–807
6. Hackney DB, Atlas SW, Grossman RI, et al. Subacute intracranial hemorrhage: contribution of spin density to appearance on spin-echo MR images. *Radiology* 1987;165:199–202
7. Barkovich AJ, Atlas SW. Magnetic resonance imaging of intracranial hemorrhage. *Radiol Clin North Am* 1988;26:801–820
8. Brooks RA, Di Chiro G, Patronas N. MR imaging of cerebral hematomas at different field strengths: theory and applications. *J Comput Assist Tomogr* 1989;13:194–206
9. Bydder GM, Pennock JM, Porteous R, Dubowitz LM, Gadian DG. MRI of intracerebral hematoma at low field (0.15T) using T2 dependent partial saturation sequences. *Neuroradiology* 1988;30:367–371
10. Di Chiro G, Brooks RA, Girton ME, et al. Sequential MR studies of intracerebral hematomas in monkeys. *AJNR: Am J Neuroradiol* 1986;7:193–199
11. Seidenwurm D, Meng T, Kowalski H, Weinreb JC, Kricheff II. Intracranial hemorrhagic lesions: evaluation with spin-echo and gradient-refocused MR imaging at 0.5 and 1.5 T. *Radiology* 1989;172: 189–194
12. Thulborn KR, Brady TJ. Iron in magnetic resonance imaging of cerebral hemorrhage. *Magn Reson Quart* 1989;5:23–38
13. Thulborn KR, Sorensen AG, Kowell NW, et al. The role of ferritin and hemosiderin in the MR appearance of cerebral hemorrhage: a histologic biochemical study in rats. *AJNR: Am J Neuroradiol* 1990;11:291–297
14. Clark RA, Watanabe AT, Bradley WG, Roberts JD. Acute hematomas: effects of deoxygenation, hematocrit, and fibrin-clot formation and retraction on T2 shortening. *Radiology* 1990;175:201–206
15. Edelman RR, Johnson K, Buxton R, et al. MR of hemorrhage: a new approach. *AJNR: Am J Neuroradiol* 1986;7:751–756
16. Thulborn KR, Atlas SW. Intracranial hemorrhage. In: Atlas SW, ed. *Magnetic resonance imaging of the brain and spine.* New York: Raven, 1991:175–224
17. Thulborn KR, Waterton JC, Matthews PM, Radda GK. Oxygenation dependence of the transverse relaxation time of water protons in whole blood at high field. *Biochim Biophys Acta* 1982;714:265–270
18. Gomori JM, Grossman RI, Yu-Ip C, Asakura T. NMR relaxation times of blood: dependence on field strength, oxidation state, and cell integrity. *J Comput Assist Tomogr* 1987;11:684–690
19. Hayman LA, Ford JF, Taber KH, Saleem A, Round ME, Bryan RN. T2 effect of hemoglobin concentration: assessment with in vitro spectroscopy. *Radiology* 1989;168:489–492
20. Hayman LA, Taber KH, Ford JJ, et al. Effect of clot formation and retraction on spin-echo MR images of blood: an in vitro study. *AJNR: Am J Neuroradiol* 1989;10:1155–1158
21. Janick PA, Hackney DB, Grossman RI, Asakura T. In vitro modeling of the magnetic resonance appearance of cerebral hemorrhage. *Magn Reson Quart* 1991;7:57–76
22. Hayman LA, Taber KH, Ford JJ, Bryan RN. Mechanisms of MR signal alteration by acute intracerebral blood: old concepts and new theories. *AJNR: Am J Neuroradiol* 1991;12:899–907
23. Wolff SD, Balaban RS. Magnetization transfer contrast (MTC) and tissue water proton relaxation in vivo. *Magn Reson Med* 1989;10: 135–144
24. Eng J, Ceckler TL, Balaban RS. Quantitative ^{1}H magnetization transfer imaging in vivo. *Magn Reson Med* 1991;17:304–314
25. Dousset V, Grossman RI, Ramer KN, et al. Experimental allergic encephalomyelitis and multiple sclerosis: lesion characterization with magnetization transfer imaging. *Radiology* 1992;182:483–491
26. Outwater E, Schnall MD, Braitman LE, Dinsmore BJ, Kressel HY. Magnetization transfer of hepatic lesions: evaluation of a novel contrast technique in the abdomen. *Radiology* 1992;182:535–540
27. Edzes HT, Samulski RT. Cross-relaxation and spin diffusion in the proton NMR of hydrated collagen. *Nature* 1977;265:521–523
28. Edzes HT, Samulski ET. The measurement of cross-relaxation in the proton NMR spin-lattice relaxation of water in biological systems: hydrated collagen and muscle. *J Magn Reson* 1978;31:207–229
29. Bryant RG, Marill K, Blackmore C, Francis C. Magnetic relaxation in blood and blood clots. *Magn Reson Med* 1990;13:133–144
30. Ceckler TL, Balaban RS. Tritium-proton magnetization transfer as a probe of cross relaxation in aqueous lipid bilayer suspensions. *J Magn Reson* 1991;93:572–588
31. Fralix TA, Ceckler TL, Wolff SD, Simon SA, Balaban RS. Lipid bilayer and water proton magnetization transfer: effect of cholesterol. *Magn Reson Med* 1991;18:214–223
32. Solomon I. Relaxation processes in a system of two spins. *Physiol Rev* 1955;99:559–565
33. Hennig J, Naureth A, Friedburg H. RARE imaging: a fast imaging method for clinical MR. *Magn Reson Med* 1986;3:823–833
34. Melki PS, Mulkern RV, Panych LP, Jolesz FA. Comparing the FAISE method with conventional dual-echo sequences. *J Magn Reson Imaging* 1991;1:319–326
35. Schnall MD, Dougherty L, Outwater E, Dousset V. Technique for magnetization transfer imaging at 1.5T using steady state pulsed saturation (abstr). In: Book of abstracts: Society of Magnetic Resonance in Medicine 1991. Vol 1. Berkeley, CA: Society of Magnetic Resonance in Medicine, 1991; 175
36. Gomori JM, Grossman RI, Schnall MD, et al. Magnetization transfer phenomena in in vitro blood. *AJNR: Am J Neuroradiol* (in press)

37. Atlas SW, Grossman RI, Gomori JM, et al. Hemorrhagic intracranial malignant neoplasms: spin-echo MR imaging. *Radiology* 1987;164:71–77
38. Brooks RA, Brunetti A, Alger JR, Di Chiro G. On the origin of paramagnetic inhomogeneity effects in blood. *Magn Reson Med* 1989;12:241–248
39. Wolff SD, Eng J, Balaban RS. Magnetization transfer contrast: method for improving contrast in gradient-recalled-echo images. *Radiology* 1991;179:133–137
40. Ordridge RJ, Helpern JA, Knight R, Welch KMA. Investigation of ischemia brain tissue using magnetization transfer contrast (MTC) imaging (abstr). In: Book of abstracts: Society of Magnetic Resonance in Medicine 1990. Vol 1. Berkeley, CA: Society of Magnetic Resonance in Medicine, 1990; 357
41. Koenig SH, Brown RD. Field cycling relaxometry of protein solutions and tissue: implications for MRI. *Prog NMR Spectroscopy* 1990;22:487–567
42. Gallier J, Rivet P, de Certaines J. ^{1}H- and ^{2}H-NMR study of bovine serum albumin solutions. *Biochim Biophys Acta* 1987;915:1–18
43. Zhong J, Gore JC, Armitage IM. Quantitative studies of hydrodynamic effects and cross-relaxation in protein solutions and tissues with proton and deuteron longitudinal relaxation times. *Magn Reson Med* 1990;13:192–203
44. DeLaPaz RL, New PFJ, Buonanno FS, et al. NMR imaging of intracranial hemorrhage. *J Comput Assist Tomogr* 1984;8:599–607
45. Gomori JM, Grossman RI, Hackney DB, Goldberg HI, Zimmerman RA, Bilaniuk LT. Variable appearances of subacute intracranial hematomas on high-field spin-echo MR. *AJNR: Am J Neuroradiol* 1987;8:1019–1026
46. Janick PA, Hackney DB, Grossman RI, Asakura T. MR imaging of various oxidation states of intracellular and extracellular methemoglobin. *AJNR: Am J Neuroradiol* 1991;12:891–897
47. Sipponen JT, Sepponen RE, Sivula A. Nuclear magnetic resonance (NMR) imaging of intracranial hemorrhage in the acute and resolving phases. *J Comput Assist Tomogr* 1983;7:954–959